Asymptotic analysis of PTT type closures for network models with variable junction concentrations

Robert D. Guy

Department of Mathematics, University of Utah, Salt Lake City, Utah 84112

Abstract

In this paper we explore variations on the PTT closure for transient network models. These models are compared for the case of a steady shear flow using asymptotic analysis for large shear rates and using numerical solutions for all shear rates. The results show that including the changing number of junctions in the closure is necessary to reproduce the behavior of the full model.

Key words: transient network models, shear thinning, Phan-Thien Tanner, closure approximation

1 Introduction

Models describing polymeric liquid follow two lines of development. In one approach a constitutive equation for the stress is used to capture observed rheological phenomena. This paper focuses on a very different approach in which the interactions between polymers are modeled and the stress is computed based on the arrangement of these polymers. This second approach yields models with multiple spatial scales, making mathematical analysis and numerical simulation difficult. By making the approximation that small-scale quantities can be replaced by their spatially averaged values, one obtains a constitutive equation that only depends on the large-scale. The goal of this paper is to quantify the impact of such closure approximations for transient network models.

Transient network models are a class of molecular models that describe polymer interactions by tracking the distribution of junctions at each point in the

Email address: guy@math.utah.edu (Robert D. Guy).

fluid. Junctions can be crosslinks or entanglements. As the fluid motion deforms the network, new junctions form and existing junctions rupture. The polymer chains which connect junctions stretch and produce stresses that are transmitted to the surrounding fluid.

The first transient network theory, due to Green and Tobolsky [1], is based on rubber elasticity. It is assumed in this model that when a junction ruptures, it immediately reforms in an equilibrium configuration. Thus, the total number of junctions is always constant. It is also assumed that the rate of breaking of a junction is a constant, independent of the strain. If it is assumed that each chain is a linear spring with zero resting length (equivalently, that the free energy of a chain is Gaussian), this first network model reduces to the Maxwell model for the stress. The Maxwell model predicts a constant shear viscosity and an elongational viscosity that is unbounded at a finite elongation rate [2].

Yamamoto [3] generalized the model of Green and Tobolsky to allow for chains with arbitrary free energy functions and a breaking rate that depends on the length of the chain. For a breaking rate that is a function of chain length, Yamamoto [4] showed that the shear viscosity is not constant, as it is in the Maxwell model. The behavior of the Yamamoto model was further explored by Fuller and Leal [5] who evaluated the solution for a variety of flows, and showed that when the breaking rate is a function of length, many more realistic behaviors are possible. However, this assumption prevents the dependence on the small scale from being eliminated, and the presence of two scales makes the model difficult to use.

Numerical techniques have been developed to simulate models of polymeric liquids containing two spatial scales. Many of these methods use stochastic simulations for the behavior on the small scale [6–8]; others solve the distribution equation on the small scale [9]. These simulations are computationally expensive, and so it is desirable to obtain a closed constitutive law that captures the essential behavior of the multiscale model.

To eliminate the dependence on the small scale, while allowing a nonconstant breaking rate, Phan-Thien and Tanner [10] assumed that the breaking rate depends on the average chain length. The average chain length at a point in space is proportional to the total energy in the stretched chains emanating from that point. This model is often called the PTT model, after the authors' initials. The closure assumption introduced in the PTT model leads to a constitutive equation, independent of the small scale, that gives more physically relevant predictions such as shear thinning and bounded extensional viscosity. The PTT model also allowed the network move relative to the local fluid velocity, but this nonaffine motion is not relevant to our current discussion.

Mewis and Denn [11] point out that it is tacitly assumed in the PTT closure model that the number of junctions remains constant. This is not the case in the two-scale Yamamoto model with a nonconstant breaking rate, and Fuller and Leal [5] point out that the changing concentration of junctions in the full model is important in capturing nonlinear phenomena. In some more recent network models the number of junctions plays a more prominent role. For example, Tanaka and Edwards [12] present a model in which the formation rate of chains decreases as a function of the concentration of active chains (chains that make up the network). In a model by Vaccaro and Marrucci [13] the concentrations of active and hanging chains are computed, and both types of chains contribute to the stress. Fogelson [14,15] developed a model of platelet aggregation which generalizes network models in that the formation rate of interplatelet links (the analog of junctions) depends on a chemical reaction which varies both spatially and temporally. In these types of models, the restriction of a constant number of junctions is inappropriate, and the original closure of the PTT model cannot be used.

In this paper we consider a more general type of PTT closure that takes into account the changing number of junctions. This closure is compared with the original PTT closure [10] and with the full model (no closure assumptions) in a steady shear flow in the asymptotic limit of increasing shear rate. The models are also compared numerically at other shear rates. The results demonstrate the importance of including the concentration of junctions in the closure as was done in [13] and [16].

The remainder of this paper is organized as follows. In section 2 the model equations are presented and the various closures are discussed. In section 3, we present the asymptotic analysis in the limit of large shear for both the full model and the closure models, and in section 4 we explore numerical comparisons for a wide range of shear rates.

2 Model Equations and Closures

The motion of the polymeric fluid is described by the incompressible Navier-Stokes equations with the addition of extra stress due to the presence of the polymer. This is written as

$$\rho\left(\boldsymbol{u}_t + \boldsymbol{u}\cdot\nabla\boldsymbol{u}\right) = -\nabla p + \mu_{\mathrm{f}}\Delta\boldsymbol{u} + \nabla\cdot\boldsymbol{\sigma}, \tag{1}$$

$$\nabla\cdot\boldsymbol{u} = 0 \tag{2}$$

where $\boldsymbol{u}$ is the velocity vector, p is the pressure, $\boldsymbol{\sigma}$ is the stress arising from polymer interactions, ρ is the fluid density, and μ_{f} is the fluid viscosity (without polymer). The network is described by a distribution function which depends

on two spatial variables: $\boldsymbol{x} = (x_1, x_2, x_3)$ is the spatial coordinate on which the other fluid variables depend, and $\boldsymbol{y} = (y_1, y_2, y_3)$ is a spatial variable that is pertinent for the much smaller scale polymer interactions. Let $\psi(\boldsymbol{x}, \boldsymbol{y}, t)d\boldsymbol{y}$ represent the concentration of chains that connect the point $\boldsymbol{x}$ to the point $\boldsymbol{x} + \boldsymbol{y}$. This distribution satisfies the equation

$$\psi_t + \boldsymbol{u} \cdot \nabla\psi + (\boldsymbol{y} \cdot \nabla\boldsymbol{u}) \cdot \nabla_y\psi = \alpha\left(\boldsymbol{x}, |\boldsymbol{y}|, t\right) - \beta\left(\boldsymbol{x}, |\boldsymbol{y}|, t\right)\psi, \tag{3}$$

where α represents the formation rate of junctions and β is the breaking rate, and it is assumed that the length scale of the chains is much smaller than the length scale associated with the fluid motion. This assumption implies that the junctions are transported on the small scale by the linearized velocity field, $\boldsymbol{y} \cdot \nabla\boldsymbol{u}$. See [17], for example, for a derivation of this equation. Equation (3) can also be written as

$$\psi_t + \boldsymbol{u} \cdot \nabla\psi + (\boldsymbol{y} \cdot \nabla\boldsymbol{u}) \cdot \nabla_y\psi = \beta\left(\boldsymbol{x}, |\boldsymbol{y}|, t\right)(\psi_0 - \psi), \tag{4}$$

where

$$\psi_0 = \frac{\alpha\left(\boldsymbol{x}, |\boldsymbol{y}|, t\right)}{\beta\left(\boldsymbol{x}, |\boldsymbol{y}|, t\right)}. \tag{5}$$

Assuming that the force in a chain is a linear function of its extension, the stress due to the stretching of the chains is given by

$$\boldsymbol{\sigma} = S_0 \int \boldsymbol{y}\boldsymbol{y}\psi \, d\boldsymbol{y}, \tag{6}$$

where S_0 is an effective stiffness parameter which depends on the temperature and the molecular weight of the polymer [2]. The product $\boldsymbol{y}\boldsymbol{y}$ is a tensor with elements $(\boldsymbol{y}\boldsymbol{y})_{ij} = y_i y_j$.

Because of the presence of two spatial scales, this system is difficult to analyze or to simulate. It is therefore desirable to obtain an equation for the stress that does not depend on the small scale variable. Multiplying equation (3) through by $S_0\boldsymbol{y}\boldsymbol{y}$ and integrating over all $\boldsymbol{y}$ gives

$$\boldsymbol{\sigma}_t + \boldsymbol{u} \cdot \nabla\boldsymbol{\sigma} = \boldsymbol{\sigma}\nabla\boldsymbol{u} + \nabla\boldsymbol{u}^{\mathrm{T}}\boldsymbol{\sigma} + a_2\boldsymbol{\delta} - \int S_0\boldsymbol{y}\boldsymbol{y}\beta\psi \, d\boldsymbol{y}, \tag{7}$$

where

$$a_2 = \int S_0\boldsymbol{y}\boldsymbol{y}\alpha\left(\boldsymbol{x}, |\boldsymbol{y}|, t\right) \, d\boldsymbol{y} = \frac{4\pi}{3}S_0\int_0^\infty \alpha(\boldsymbol{x}, r, t)r^4 \, dr, \tag{8}$$

and $\boldsymbol{\delta}$ represents the identity tensor. If the breaking rate, β, is a function of the length of the chain, this procedure does not yield an equation for the stress that is independent of the small scale. However, if the breaking rate does not depend on the length of the chain, equation (7) simplifies to

$$\boldsymbol{\sigma}_t + \boldsymbol{u} \cdot \nabla\boldsymbol{\sigma} = \boldsymbol{\sigma}\nabla\boldsymbol{u} + \nabla\boldsymbol{u}^{\mathrm{T}}\boldsymbol{\sigma} + a_2\boldsymbol{\delta} - \beta\boldsymbol{\sigma}, \tag{9}$$

and the small scale is eliminated. A similar derivation starting with equation (4) gives

$$\boldsymbol{\sigma}_t + \boldsymbol{u} \cdot \nabla \boldsymbol{\sigma} = \boldsymbol{\sigma} \nabla \boldsymbol{u} + \nabla \boldsymbol{u}^{\mathrm{T}} \boldsymbol{\sigma} + \beta \left(\sigma_0 \boldsymbol{\delta} - \boldsymbol{\sigma} \right), \tag{10}$$

where

$$\sigma_0 = \int S_0 \boldsymbol{y}\boldsymbol{y} \psi_0 \, d\boldsymbol{y} = \frac{4\pi}{3} S_0 \int_0^\infty \psi_0 r^4 \, dr. \tag{11}$$

Even though equations (3) and (4) are equivalent, depending on the closure, equations (9) and (10) may not be. This is discussed in more detail below.

A constant breaking rate, $\beta = \beta_0$, is clearly one assumption that leads to a closed constitutive law. In this case, equations (9) and (10) are equivalent, and they reduce to the upper convected Maxwell equation (after the subtraction of the equilibrium, isotropic stress) [2]. In order to produce a constitutive law that is independent of the small scale without the restriction of a constant breaking rate, Phan-Thien and Tanner [10] assumed that the breaking rate at each point $\boldsymbol{x}$ depends on the trace of the stress at $\boldsymbol{x}$ rather than on the length of the chain. The trace of the stress equals the total energy due to stretching of chains emanating from $\boldsymbol{x}$. Using this assumption, equation (9) becomes

$$\boldsymbol{\sigma}_t + \boldsymbol{u} \cdot \nabla \boldsymbol{\sigma} = \boldsymbol{\sigma} \nabla \boldsymbol{u} + \nabla \boldsymbol{u}^{\mathrm{T}} \boldsymbol{\sigma} + a_2 \boldsymbol{\delta} - \beta \left(\mathrm{Tr}(\boldsymbol{\sigma}) \right) \boldsymbol{\sigma}, \tag{12}$$

and equation (10) becomes

$$\boldsymbol{\sigma}_t + \boldsymbol{u} \cdot \nabla \boldsymbol{\sigma} = \boldsymbol{\sigma} \nabla \boldsymbol{u} + \nabla \boldsymbol{u}^{\mathrm{T}} \boldsymbol{\sigma} + \beta \left(\mathrm{Tr}(\boldsymbol{\sigma}) \right) \left(\sigma_0 \boldsymbol{\delta} - \boldsymbol{\sigma} \right). \tag{13}$$

Equation (13) corresponds to the original PTT closure, and it is not equivalent to equation (12). We refer to the constitutive equation (12) as PTT*.

To see the difference in closure models and its consequences, consider the concentration of junctions defined by

$$z = \int \psi \, d\boldsymbol{y}. \tag{14}$$

An evolution equation for z can be generated by integrating equation (3) or (4) over all $\boldsymbol{y}$, and using the PTT closure assumption. The resulting equations are

$$z_t + \boldsymbol{u} \cdot \nabla z = a_0 - \beta \left(\mathrm{Tr}(\boldsymbol{\sigma}) \right) z, \tag{15}$$

from (3), and

$$z_t + \boldsymbol{u} \cdot \nabla z = \beta \left(\mathrm{Tr}(\boldsymbol{\sigma}) \right) (z_0 - z), \tag{16}$$

from (4), where

$$a_0 = \int \alpha \left(\boldsymbol{x}, |\boldsymbol{y}|, t \right) \, d\boldsymbol{y} = 4\pi \int_0^\infty \alpha(\boldsymbol{x}, r, t) r^2 \, dr, \tag{17}$$

and z_0 is defined similarly.

Suppose that all variables and parameters are homogeneous in $\boldsymbol{x}$ and the formation and breaking rates are independent of time. Assume also that the network is initially at its equilibrium state without flow, and then the flow is started. Under these conditions, equation (16) predicts that $z \equiv z_0$ for all time, and so the concentration of junctions does not change. On the other hand, equation (15) implies that the concentration of junctions does not remain constant for all time. This example demonstrates that the two constitutive equations (12) and (13) are not equivalent, but does not show that the resulting stresses differ significantly. The differences in the stresses are explored in detail in the later sections of this paper.

One interpretation of the original PTT closure is that the breaking rate is assumed to be a function of the average squared chain length rather than the actual chain length. The average squared chain length, $\langle y^2 \rangle$, is given by

$$\langle y^2 \rangle = \frac{\int y^2 \psi \, d\boldsymbol{y}}{\int \psi \, d\boldsymbol{y}} = \frac{1}{S_0} \frac{\mathrm{Tr}(\boldsymbol{\sigma})}{z}. \tag{18}$$

Note that if z is constant, as it is in the original PTT closure, then $\mathrm{Tr}(\boldsymbol{\sigma}) \propto \langle y^2 \rangle$. However, if z is not constant as with the PTT* closure, then the average squared length is not proportional to the trace of the stress. In this case a possibly more appropriate closure is obtained by replacing equation (12) with the equations

$$\boldsymbol{\sigma}_t + \boldsymbol{u} \cdot \nabla \boldsymbol{\sigma} = \boldsymbol{\sigma} \nabla \boldsymbol{u} + \nabla \boldsymbol{u}^{\mathrm{T}} \boldsymbol{\sigma} + a_2 \boldsymbol{\delta} - \beta \left(\frac{\mathrm{Tr}(\boldsymbol{\sigma})}{z} \right) \boldsymbol{\sigma} \tag{19}$$

$$z_t + \boldsymbol{u} \cdot \nabla z = a_0 - \beta \left(\frac{\mathrm{Tr}(\boldsymbol{\sigma})}{z} \right) z \tag{20}$$

This is the type of closure considered in [13] and [16] in network type models for which the number of junctions must not be constant. We refer to this closure as PTT-vj, the letters vj representing *variable junctions*, because the concentration of junctions is allowed to vary and appears explicitly in the closure.

In the next section we compare the behavior of the three different PTT type closures: the original PTT model from equation (13), the PTT* model from (12), and the PTT-vj model from equations (19) and (20). The steady state shear viscosity in the limit of large shear rate obtained from the three closures is compared with that from the model without making additional closure assumptions.

3 Shear Flow – Asymptotic Analysis

In order to compare the different closures discussed in the previous section with the full model (model without closure assumptions) we examine the predicted shear viscosity in a steady state shear flow in the limit of a large shear rate. Suppose that the velocity field is the steady, linear shear flow

$$\boldsymbol{u} = (\gamma x_2, 0, 0)\,, \tag{21}$$

where γ is the shear rate. The shear viscosity is defined as

$$\mu = \frac{\sigma_{12}}{\gamma}. \tag{22}$$

Suppose that the network is homogeneous in $\boldsymbol{x}$ and the distribution is in steady state. Additionally, assume that the formation and breaking rate functions depend only on the length of the chain.

3.1 Full Model

Equation (3) for the distribution of junctions reduces to

$$\gamma y_2 \frac{\partial \psi}{\partial y_1} = \alpha\left(|\boldsymbol{y}|\right) - \beta\left(|\boldsymbol{y}|\right)\psi. \tag{23}$$

The solution to this equation can easily be expressed as an integral, and asymptotic analysis can be performed in the limit of a large shear rate. This analysis is performed in [4] and [16] for the cases when the breaking rate is asymptotic to a monomial in the length of the chain. Suppose that the breaking rate can be written as

$$\beta = \left(\kappa_{L}\,|\boldsymbol{y}|\right)^n + \text{lower order terms}. \tag{24}$$

The constant κ_L represents a scale factor. The shear viscosity to leading order is then

$$\mu = C_n \gamma^{-2n/(n+1)} + o\left(\gamma^{-2n/(n+1)}\right), \tag{25}$$

where

$$C_n = \frac{\kappa_L^{-2n/(n+1)}}{(n+1)^{(n-1)/(n+1)}}\Gamma\left(\frac{2}{n+1}\right)\frac{4\pi S_0(n+1)}{(n+3)}\int_0^\infty \alpha\left(r\right) r^{\frac{2n+4}{n+1}}\,dr. \tag{26}$$

Although this asymptotic result is only available for polynomial breaking rates, it can be shown that in the case where all chains must break before reaching some critical length (the breaking rate has a vertical asymptote), the shear viscosity behaves like

$$\mu = \mathcal{O}\left(\gamma^{-2}\right), \tag{27}$$

and this gives the maximum possible rate of shear thinning. We note that the order of the shear viscosity in the limit of large shear was given in [18] using scaling arguments, but the asymptotic constant was not computed.

3.2 Original PTT Model – Equation (13)

First we examine the original PTT closure model for which the concentration of junctions is constant. The constitutive equation is

$$0 = \boldsymbol{\sigma}\nabla\boldsymbol{u} + \nabla\boldsymbol{u}^{\mathrm{T}}\boldsymbol{\sigma} + \beta\left(T\right)\left(\sigma_0\boldsymbol{\delta} - \boldsymbol{\sigma}\right), \tag{28}$$

where, for simplicity, we have denoted the trace of the stress by T. An isotropic, constant stress proportional to σ_0 can be subtracted from the stress. This change only modifies the definition of the pressure, but does not change the viscosity. Let

$$\boldsymbol{\tau} = \boldsymbol{\sigma} - \sigma_0\boldsymbol{\delta}. \tag{29}$$

In terms of $\boldsymbol{\tau}$, equation (28) becomes

$$0 = \boldsymbol{\tau}\nabla\boldsymbol{u} + \nabla\boldsymbol{u}^{\mathrm{T}}\boldsymbol{\tau} - \beta\left(T\right)\boldsymbol{\tau} + \sigma_0\left(\nabla\boldsymbol{u} + \nabla\boldsymbol{u}^{\mathrm{T}}\right). \tag{30}$$

The equations in component form are

$$0 = 2\gamma\tau_{12} - \beta(T)\tau_{11} \tag{31}$$
$$0 = -\beta(T)\tau_{22} \tag{32}$$
$$0 = -\beta(T)\tau_{33} \tag{33}$$
$$0 = \gamma\sigma_0 + \gamma\tau_{22} - \beta(T)\tau_{12}, \tag{34}$$

Since $\tau_{22} = \tau_{33} = 0$, the trace of this new stress is simply τ_{11}. Solving for the nonzero components in terms of β and γ gives

$$\tau_{11} = \frac{2\sigma_0\gamma^2}{\beta^2} \tag{35}$$
$$\tau_{12} = \frac{\sigma_0\gamma}{\beta}. \tag{36}$$

Suppose that the breaking rate is a function of the trace of $\boldsymbol{\tau}$ rather than $\boldsymbol{\sigma}$, and let $\hat{T}$ denote this trace. The solution in terms of $\hat{T}$ and γ is

$$\tau_{11} = \hat{T} \tag{37}$$
$$\tau_{12} = \left(\frac{\sigma_0}{2}\right)^{1/2}\hat{T}^{1/2}, \tag{38}$$

and so the viscosity is

$$\mu = \left(\frac{\sigma_0}{2}\right)^{1/2}\hat{T}^{1/2}\gamma^{-1}. \tag{39}$$

Without specifying the form of the breaking rate, equation (39) provides some insight. Combining (35) and (37) and solving for γ^2 gives

$$\gamma^2 = \frac{\beta^2 \hat{T}}{2\sigma_0}. \tag{40}$$

As $\gamma \to \infty$, this equation shows that at least one of β or $\hat{T}$ must grow without bound. It is physically unreasonable that the breaking rate could become unbounded as the trace became small. Therefore the trace cannot approach zero as γ gets large. Thus, equation (39) shows that the shear viscosity decreases no faster than γ^{-1}. Comparing this result with the full model shows that this closure is incapable of capturing all the possible behaviors of the full model.

In Table A.1 we give the leading order term of the shear viscosity for three types of breaking rates: power-law, exponential, and finite trace. The quantity κ_T that appears in each of the models is simply scale factor for the trace in the breaking rate function. In the finite trace breaking rate, the quantity $T_{\max}$ represents the upper bound for the trace. The details of the computation are similar for the three closure models, and so we present them for PTT-vj only. As can be seen from these results, a power-law breaking rate function can give any power-law rate of shear thinning below maximal rate of γ^{-1}. The exponential and the finite trace breaking rates have similar asymptotic behaviors, except that the viscosity predicted by the exponential breaking decreases slightly more slowly than the maximal rate predicted by the finite trace breaking. As stated before, this closure cannot reproduce the range of shear viscosities from the full model.

The asymptotic shear viscosities for the original PTT model were also computed by Tanner [19] for linear and exponential breaking rates. Our power-law results agree with this result with the appropriate change in scale ($\kappa_T = \epsilon/\mu_0$ and $\sigma_0 = \mu_0/\lambda$). However the result given in [19] for the exponential breaking rate is missing the logarithmic term that appears in the leading order term we computed. How this logarithmic term arises can be seen in the computation for the PTT-vj model in section 3.4.2.

3.3 PTT – Equation (12)*

The PTT* closure model is a slight variation on the original PTT model. The main difference is that the concentration of junctions is not fixed. In this section we show that this closure model gives different behavior from the original PTT closure model. The constitutive equation is

$$0 = \boldsymbol{\sigma}\nabla\boldsymbol{u} + \nabla\boldsymbol{u}^{\mathrm{T}}\boldsymbol{\sigma} + a_2\boldsymbol{\delta} - \beta\left(T\right)\boldsymbol{\sigma}, \tag{41}$$

The equations for the components of the stress are

$$0 = 2\gamma\sigma_{12} + a_2 - \beta(T)\sigma_{11} \tag{42}$$
$$0 = a_2 - \beta(T)\sigma_{22} \tag{43}$$
$$0 = a_2 - \beta(T)\sigma_{33} \tag{44}$$
$$0 = \gamma\sigma_{22} - \beta(T)\sigma_{12} \tag{45}$$

Before specifying the form of the breaking rate function, it is useful to manipulate these equations. Solving equations (42)–(45) for the stresses in terms of β and γ gives

$$\sigma_{11} = \frac{\beta^2 + 2\gamma^2}{\beta^3} a_2 \tag{46}$$
$$\sigma_{22} = \sigma_{33} = \frac{a_2}{\beta} \tag{47}$$
$$\sigma_{12} = \frac{a_2}{\beta^2}\gamma. \tag{48}$$

The shear viscosity is

$$\mu = \frac{a_2}{\beta^2}, \tag{49}$$

and the trace is

$$T = \frac{3\beta^2 + 2\gamma^2}{\beta^3} a_2. \tag{50}$$

Solving the last equation for γ^2 gives

$$\gamma^2 = \frac{\beta^3 T}{2a_2} - \frac{3}{2}\beta^2. \tag{51}$$

Note that as $\gamma^2 \to \infty$, equation (51) shows that at least one of β or T must grow without bound. We will assume that β grows without bound, but that T may be bounded. For large enough γ, the second term in equation (51) becomes small compared to the first. Ignoring this term gives

$$\gamma^2 \approx \frac{\beta^3 T}{2a_2}. \tag{52}$$

Once the form of β is specified, equation (52) can be inverted to find T in terms of γ. Also using equation (52), the stress can be expressed in terms of T rather than β. Equations (46)–(49) become

$$\sigma_{11} \approx T - (2a_2)^{-1/3}\gamma^{-2/3}T^{1/3} \approx T \tag{53}$$
$$\sigma_{22} = \sigma_{33} \approx 2^{-1/3}a_2^{2/3}\gamma^{-2/3}T^{1/3} \tag{54}$$
$$\sigma_{12} \approx 2^{-2/3}a_2^{1/3}\gamma^{-1/3}T^{2/3} \tag{55}$$
$$\mu \approx 2^{-2/3}a_2^{1/3}\gamma^{-4/3}T^{2/3}. \tag{56}$$

As was argued for the previous model, equation (56) shows that the viscosity can decrease no faster than at a rate proportional to $\gamma^{-4/3}$. The leading order terms of the viscosity for three different forms of the breaking rate are shown in Table A.2. As with the original PTT model, the quantity κ_T represents a scale factor for the trace, and $T_{\max}$ is the upper bound for the trace in the finite trace breaking rate. The results are similar to those for the original PTT. That is, the power-law breaking rate functions can produce shear thinning of all powers below the maximal rate of $\gamma^{-4/3}$, the finite trace model predicts the maximum rate of shear thinning, and the exponential predicts an almost maximal rate of shear thinning. This closure is also incapable of reproducing the range of possible behaviors of the full model.

3.4 PTT-vj – Equations (19)–(20)

In the previous two sections we showed that the PTT closure and the PTT* cannot match the range of shear thinning rates of the full model. The PTT* does not fix the concentration of junctions, but this information is not included in the closure as it is in the PTT-vj closure. In this section we analyze the behavior of the the PTT-vj closure. The equations are

$$0 = \boldsymbol{\sigma}\nabla\boldsymbol{u} + \nabla\boldsymbol{u}^{\mathrm{T}}\boldsymbol{\sigma} + a_2\boldsymbol{\delta} - \beta\left(\frac{T}{z}\right)\boldsymbol{\sigma} \tag{57}$$

$$0 = a_0 - \beta\left(\frac{T}{z}\right)z. \tag{58}$$

The equations for the components are

$$0 = 2\gamma\sigma_{12} + a_2 - \beta\left(\frac{T}{z}\right)\sigma_{11} \tag{59}$$

$$0 = a_2 - \beta\left(\frac{T}{z}\right)\sigma_{22} \tag{60}$$

$$0 = a_2 - \beta\left(\frac{T}{z}\right)\sigma_{33} \tag{61}$$

$$0 = \gamma\sigma_{22} - \beta\left(\frac{T}{z}\right)\sigma_{12} \tag{62}$$

$$0 = a_0 - \beta\left(\frac{T}{z}\right)z. \tag{63}$$

Equation (63) immediately relates the concentration of junctions to the breaking rate by

$$\beta = \frac{a_0}{z}. \tag{64}$$

Using this relationship, the stresses and viscosity can be expressed as functions of the concentration of junctions and the shear rate:

$$\sigma_{11} = \frac{a_2}{a_0}\left(z + \frac{2\gamma^2}{a_0^2}z^3\right) \tag{65}$$

$$\sigma_{22} = \sigma_{33} = \frac{a_2}{a_0}z \tag{66}$$

$$\sigma_{12} = \frac{a_2\gamma}{a_0^2}z^2 \tag{67}$$

$$\mu = \frac{a_2}{a_0^2}z^2. \tag{68}$$

Equation (51) for the PTT* closure holds for this closure as well, and combining this with equation (64) gives

$$\gamma^2 = \frac{a_0^3 T}{2a_2 z^3} - \frac{3a_0^2}{2z^2}. \tag{69}$$

For the different forms of β, we use equation (64) to find the trace as a function of z. Then equation (69) can be inverted to find z as a function of γ, and this expression for z is substituted into equations (65)–(68) to find the stresses and viscosity.

3.4.1 Power-Law Breaking

Suppose the breaking rate is of the form

$$\beta = \left(\kappa_L^2 \frac{T}{z}\right)^n. \tag{70}$$

The constant κ_L represents a scale factor for length, as in the full model. Because the trace per junction (T/z) has units of length squared, the quantity κ_L^2 appears as the scale factor in this model. Using equation (64) to find T as a function of z gives

$$T = \frac{a_0^{1/n}}{\kappa_L^2} z^{(n-1)/n}. \tag{71}$$

Plugging this into equation (69) gives

$$\gamma^2 = \frac{a_0^{(3n+1)/n}}{2a_2\kappa_L^2 z^{(2n+1)/n}} - \frac{3a_0^2}{2z^2}. \tag{72}$$

The leading order solution to this equation is

$$z = \left(\frac{2a_2\kappa_L^2}{a_0^{(3n+1)/n}}\right)^{-n/(2n+1)} \gamma^{-2n/(2n+1)} + o\left(\gamma^{-2n/(2n+1)}\right). \tag{73}$$

Using this expression in (68) gives the leading order behavior of the shear viscosity

$$\mu = \left(\frac{a_0 a_2^{1/2n}}{2\kappa_L^2} \right)^{2n/(2n+1)} \gamma^{-4n/(2n+1)} + o\left(\gamma^{-4n/(2n+1)}\right). \tag{74}$$

Note that the range of shear thinning rates agrees with the range predicted by the full model.

3.4.2 Exponential Breaking

Suppose that the breaking rate is

$$\beta = \exp\left(\kappa_L^2 T/z\right). \tag{75}$$

As for power-law breaking, we use equation (64) to find T as a function of z to obtain

$$T = \frac{z}{\kappa_L^2} \ln\left(\frac{a_0}{z}\right). \tag{76}$$

Substituting this expression for T into equation (69) gives

$$\gamma^2 = \frac{a_0^3}{2\kappa_L^2 a_2 z^2} \ln\left(\frac{a_0}{z}\right) - \frac{3a_0^2}{2z^2}. \tag{77}$$

As $\gamma \to \infty$, z must go to zero, and the second term on the right side of this equation grows more slowly than the first. In order to find the leading order behavior, it is sufficient to solve the equation

$$\gamma^2 = \frac{a_0^3}{2\kappa_L^2 a_2 z^2} \ln\left(\frac{a_0}{z}\right) \tag{78}$$

to find z as a function of γ. Before doing this, we introduce a change of variables

$$g^2 = \frac{2\kappa_L^2 a_2}{a_0} \gamma^2; \qquad w = \frac{a_0}{z}. \tag{79}$$

The equation we wish to solve is

$$g^2 = w^2 \ln(w). \tag{80}$$

We seek to solve this equation to leading order as $w \to \infty$. Take the logarithm of this equation and introduce the change of variables

$$h = \ln(g); \qquad x = \ln(w) \tag{81}$$

to obtain

$$2h = 2x + \ln(x). \tag{82}$$

For large x, $2x$ dominates the right side of equation (82), and so we may write

$$x = h + h_1, \qquad h_1 = o(h). \tag{83}$$

This is substituted into equation (82) in order to find an expansion of h_1. After some minor manipulations,

$$h_1 = -\frac{1}{2}\ln(h) - \frac{1}{2}\ln\left(1 + \frac{h_1}{h}\right). \tag{84}$$

Because $h_1 = o(h)$, the second logarithm must go to zero as h gets large, and so the two-term expansion is

$$x = h - \frac{1}{2}\ln(h) + h_2, \qquad h_2 = o\Big(\ln(h)\Big). \tag{85}$$

Note that the first two terms are large when h is large. We must continue expanding until the last term goes to zero for large h. This is a consequence of the change of variables, since the expansion must be exponentiated when changing back to the original variables, and therefore transforms into a product of exponentials. The only way the error terms can be ignored is if the corresponding terms in the series for x go to zero in the asymptotic limit, so that when exponentiated they multiply the asymptotic approximation by one. Substituting (85) into (82) to find h_2, we obtain after some manipulation

$$h_2 = \frac{\ln(h)}{4h} + o\left(\frac{\ln(h)}{h}\right). \tag{86}$$

Because $h_2 \to 0$ as $h \to 0$, no other terms are needed to find the leading order behavior of the original variables.

The expansion of x is

$$x = h - \frac{1}{2}\ln(h) + \frac{\ln(h)}{4h} + o\left(\frac{\ln(h)}{h}\right), \tag{87}$$

and we wish to express this in terms of the original variables. First change back to the variables w and g and exponentiate the series to get

$$w = g\Big(\ln(g)\Big)^{-1/2} \exp\left(\frac{\ln\Big(\ln(g)\Big)}{4\ln(g)} + o\left(\frac{\ln\Big(\ln(g)\Big)}{\ln(g)}\right)\right). \tag{88}$$

To leading order this gives,

$$w = g\Big(\ln(g)\Big)^{-1/2} + \mathcal{O}\left(\frac{g\ln\Big(\ln(g)\Big)}{\Big(\ln(g)\Big)^{3/2}}\right). \tag{89}$$

Now changing back to the original variables of z and γ, we obtain

$$z = \left(\frac{a_0^3}{2\kappa_L^2 a_2}\right)^{1/2} \gamma^{-1} \left(\ln(\gamma) - \frac{1}{2}\ln\left(\frac{a_0}{2\kappa_L^2 a_2}\right)\right)^{1/2} + \mathcal{O}\left(\frac{\ln\Big(\ln(\gamma)\Big)}{\gamma\Big(\ln(\gamma)\Big)^{1/2}}\right). \quad (90)$$

Using this expression for z in equation (68), the leading order behavior of the viscosity is

$$\mu = \frac{a_0}{2\kappa_L^2}\gamma^{-2}\left(\ln(\gamma) - \frac{1}{2}\ln\left(\frac{a_0}{2\kappa_L^2 a_2}\right)\right) + o\left(\gamma^{-2}\ln(\gamma)\right). \quad (91)$$

3.4.3 Breaking at Finite Length

Suppose the breaking rate is of the form

$$\beta = \frac{1}{\kappa_L^2\left(L_{\max}^2 - T/z\right)}. \quad (92)$$

The quantity $L_{\max}^2$ represents an upper bound for T/z. This notation is used because T/z has units of length squared. Solving equation (64) for T in terms of z gives

$$T = L_{\max}^2 z - \frac{1}{a_0\kappa_L^2}z^2, \quad (93)$$

and substituting this into equation (69) yields the relation between γ^2 and z

$$\gamma^2 = \left(\frac{a_0^3 L_{\max}^2}{2a_2} - \frac{3a_0^2}{2}\right)\frac{1}{z^2} - \frac{a_0^2\kappa_L^2}{2a_2}\frac{1}{z}. \quad (94)$$

This equation is quadratic in z and can be solved exactly, but we solve for the leading order term for large γ instead, and obtain

$$z = \left(\frac{a_0^3 L_{\max}^2 - 3a_2 a_0^2}{2a_2}\right)^{1/2}\gamma^{-1} + o\left(\gamma^{-1}\right). \quad (95)$$

This implies that the leading order shear viscosity is

$$\mu = \left(\frac{a_0 L_{\max}^2 - 3a_2}{2}\right)\gamma^{-2} + o\left(\gamma^{-2}\right) \quad (96)$$

Note that here the maximal rate of shear thinning agrees with the maximal rate predicted by the full model when the links are restricted to have finite length. In summary the shear viscosities for the three different breaking rates are given in Table A.3.

4 Comparison

The asymptotic results from the previous section show that only the closure PTT-vj, which includes the number of junctions, is capable of reproducing the range of shear thinning rates predicted by the full model. In this section we compare the results from the full model with the results of the PTT-vj closure. First we examine the differences in the asymptotic result for the power-law breaking rate for the two models, and second, we present numerical comparison for a wide range of shear rates.

So far the results have been presented in terms of dimensional variables. The number of parameters can be reduced by nondimensionalizing the equations, and this makes the numerical comparison more straightforward. Let r_0 represent the characteristic length scale of the links, and scale the microscale lengths by this quantity. Let α_0 and β_0 represent characteristic formation rate and breaking rate scales, respectively. For the full model, scale the junction concentration by α_0/β_0 and the stress by $S_0 r_0^5 \alpha_0/\beta_0$. Finally scale the shear rate by β_0.

4.1 Asymptotic Comparison

We compare the asymptotic shear viscosities for the full model and the PTT-vj closure model for the power-law breaking rates

$$\beta_{\text{full}} = (\kappa_L r)^{2n}; \qquad \beta_{\text{close}} = \left(\kappa_L^2 \frac{T}{z}\right)^n. \tag{97}$$

In the nondimensionalization the constant S_0 is part of the stress scale, making the quantity T/z equal to the nondimensional average squared link length, so this comparison amounts to replacing squared link length with its average in the breaking rate function.

The shear viscosities in (25) (with n replaced by $2n$) and (74) show that the two breaking rates in (97) produce the same shear thinning rate to leading order but with different proportionality constants. In order to investigate what influences the difference in the proportionality constants, we examine the ratio

$$\frac{\mu_{\text{full}}}{\mu_{\text{close}}} = 6^{1/(2n+1)} \frac{(2n+1)}{(2n+3)} \left(\frac{2}{2n+1}\right)^{(2n-1)/(2n+1)} \Gamma\left(\frac{2}{2n+1}\right) A_n, \tag{98}$$

where

$$A_n = \frac{\displaystyle\int r^{(4n+4)/(2n+1)} \alpha(r)\, dr}{\displaystyle\left(\int r^4 \alpha(r)\, dr\right)^{1/(2n+1)} \left(\int r^2 \alpha(r)\, dr\right)^{2n/(2n+1)}}. \tag{99}$$

The quantity A_n contains all the dependence on the formation rate function.

For the Gaussian formation rate

$$\alpha(r) = \exp\left(-r^2\right), \tag{100}$$

the value of A_n is

$$A_n = \frac{2^{(2n+2)/(2n+1)}}{3^{1/(2n+1)}\pi^{1/2}}\Gamma\left(\frac{6n+5}{4n+2}\right). \tag{101}$$

Note that this quantity is independent of the scale of the formation rate and of the width of the Gaussian. A plot of (101) is displayed in Fig.A.1, and shows that for $n \geq 1$, A_n is an increasing function of n, which approaches 1 as n grows. We also computed A_n for breaking rates of the form

$$\alpha(r) = \left(1 - r^b\right) H(1-r), \tag{102}$$

where $H(x)$ is the Heaviside function, and found the results similar to those for the Gaussian. Therefore for sharply increasing breaking rates, the form of the formation rate function does not significantly affect the value of A_n.

Now compare the portion of the the ratio in (98) that is independent of the formation rate function. Its value ranges between 1 and approximately 1.3 and approaches 1 for large n. The closure model results from replacing squared length with average squared length. We could instead replace squared length by some multiple of average squared length, the multiple being chosen so that the asymptotic behavior of the shear viscosity is identical to that of the full model. Call the multiplicative constant C_a, so that the closure model results from the substitution

$$r^2 \longrightarrow C_a \langle r^2 \rangle. \tag{103}$$

This modifies the closure breaking rate (97), so that

$$\beta_{\text{close}} = C_a^n \left(\kappa_L^2 \frac{T}{z}\right)^n. \tag{104}$$

Assuming that $A_n \approx 1$, meaning the closure is nearly independent of the geometry of the formation rate function, and then defining

$$C_a = \left(\frac{\mu_{\text{close}}}{\mu_{\text{full}}}\right)^{(2n+1)/2n}, \tag{105}$$

would produce a closure whose asymptotic shear viscosity matches that of the full model.

4.2 Numerical Comparison

First we verify the asymptotic shear viscosities (25) and (74) for the case of a quadratic breaking rate. Other power laws were verified as well, but the results are not presented. For simplicity of computation we use the formation rate

$$\alpha(r) = \begin{cases} 1 & \text{if } r \leq 1 \\ 0 & \text{if } r > 1 \end{cases}. \tag{106}$$

It is a reasonable assumption that the breaking rate should vary little over the range of lengths at which links form, but increase as a power law for large r. A simple breaking rate satisfying these requirements is

$$\beta(r) = \begin{cases} 1 & \text{if } r \leq 1 \\ r^2 & \text{if } r > 1 \end{cases}. \tag{107}$$

For the full model, we computed the shear viscosity numerically by first solving (23) for ψ and then integrating the result to find the shear stress. For the closure model, equations (59)–(63) are solved for each shear rate using Newton's method. The breaking rate used for the closure is

$$\beta\left(\frac{T}{z}\right) = \begin{cases} 1 & \text{if } T/z \leq 1 \\ T/z & \text{if } T/z > 1 \end{cases}. \tag{108}$$

The asymptotic results are compared with the numerical results in Fig.A.2 for both models. These plots verify the asymptotic forms for the shear viscosities derived in the paper. The asymptotic viscosity is very close to the actual viscosity for the full model for shear rate above about 30 (nondimensional) and for the closure model above shear rate 10.

Next we compare the shear viscosity obtained from the full model and the closure model to each other for shear rates both large and small. Fig.A.3 shows these results. Note that both models show the same power-law dependence on the shear rate, as predicted by the asymptotics, but the constant multiple is larger for the full model, also predicted by the asymptotics. The results are notably different around shear rate 1. The full model begins shear thinning at a much lower shear rate than the closure model.

To understand why the full model and closure model begin shear thinning at different rates, we examine the closure model at low shear. Equations (57) and

(58) at zero shear rate give the trace and concentration of junctions as

$$T = 3a_2/\beta\,(T/z) \tag{109}$$
$$z = a_0/\beta\,(T/z)\,. \tag{110}$$

Note that the ratio T/z is independent of the breaking rate function. Using the formation rate (106) and the definitions of the constants a_2 and a_0 given by (8) and (17) respectively, the average bond length at zero shear rate is

$$\langle r^2 \rangle = \frac{T}{z} = \frac{\int_0^\infty \alpha(r) r^4\, dr}{\int_0^\infty \alpha(r) r^2\, dr} = \frac{3}{5}. \tag{111}$$

Rather than simply replacing the squared length with the average squared length in (107), we try the closure breaking rate

$$\beta\left(\frac{T}{z}\right) = \begin{cases} 1 & \text{if } \; T/z \leq 3/5 \\ 1 + T/z - 3/5 & \text{if } \; T/z > 3/5 \end{cases}. \tag{112}$$

The full model breaking rate (107) is constant below the length at which links form, and the closure (112) results from assuming that the closure breaking rate is constant up to the average length at which links form. The shear viscosity from this closure are compared with the full model in Fig.A.4. This breaking rate shows much better agreement with the full model and low and moderate shear rates compared to the closure with breaking rate (108).

Finally we compare the shear viscosities produced by the exponential breaking rate. The formation rate used is again (106). For the full model the breaking rate tested is

$$\beta(r) = \begin{cases} 1 & \text{if } \; r \leq 1 \\ \exp\Big(0.5(r^2 - 1)\Big) & \text{if } \; r > 1 \end{cases}. \tag{113}$$

The result is compared with the shear viscosity produced by the closure model with breaking rate

$$\beta(r) = \begin{cases} 1 & \text{if } \; T/z \leq 3/5 \\ \exp\Big(0.5\,(T/z - 3/5)\Big) & \text{if } \; T/z > 3/5 \end{cases}. \tag{114}$$

The results are displayed in Fig.A.5. The asymptotic approximation is in excellent agreement with the closure model. The full model viscosity is slightly larger than that of the closed model at high shear. Recall this was also the case with the power-law breaking rate. Overall there is excellent agreement between the closure model and the full model at all shear rates.

5 Conclusions

In this paper we examine variations on the PTT closure for transient network models. The original PTT model forces the concentration of junctions to remain constant, but this is not the case for the multiple scale model without closure assumptions for a nonconstant breaking rate. We examine variations on the original closure in which the number of junctions does not remain constant. Each of these closures produces different results, as is demonstrated by the asymptotic analysis of the shear viscosity for large shear rate.

The closure in which the breaking rate depends on the ratio of the trace of the stress to the concentration of junctions, called PTT-vj in this paper, amounts to replacing length with average length. This is also true in the original PTT closure, but PTT-vj does not fix the concentration of junctions. The PTT-vj closure is the only closure that is capable of reproducing all of the possible shear thinning rates predicted by the full model. Numerical tests show that this closure can capture the shear viscosity predicted by the full model for all shear rates, provided the closure breaking rate is chosen appropriately.

In some recent variations on network models, the number of junctions appears as an essential part of the model. The results of this paper demonstrate the importance of utilizing the number of junctions in closure approximations for transient network type models. The closure model that included the number of junctions did an excellent job of reproducing the shear viscosity of the full model. Further analysis and explorations of the performance of the closure model under different conditions, such as transient flows and elongational flows, are necessary to fully understand the limitations and utility of such closures. Some numerical comparisons are made in [16] for transient elongational flows in which the concentration of polymer varies spatially.

Similar closure problems arise in other multiscale models of complex fluids. One such example is the FENE (Finitely Extensible Non-linear Elastic) dumbbell model [17]. In the FENE model the closure problem arises due to a nonlinear force law. The idea of replacing length squared with average length squared is used in these models as well, giving the FENE-P model. This closure reproduces some behavior of the full FENE model in steady flows, but shows some differences in transient flows [20,21]. Lielens et al. [22,23] developed a closure model that improves on the FENE-P model in that the closure depends on average quantities in addition to the average length. Similar ideas may be extended to transient network models in the future. We note that a major difference between network models and dumbbell models is that the number of dumbbells does not change in time. As we have argued in this work, the number of junctions must be included in closure models for network models.

Acknowledgements

This author would like to thank Aaron Fogelson and James Keener for helpful discussions related to this work. This work was supported in part by an NSF VIGRE grant and NSF grant #DMS-1039926.

A Full Model– Power-Law Breaking

A sketch of the derivation of equation (25) is presented in this appendix. More detailed arguments are presented in [16].

We begin by assuming that the formation function $\alpha(|\boldsymbol{y}|)$ has compact support, meaning that there is some radius beyond which no links form. Let $r = |\boldsymbol{y}|$. Scale the lengths by the size of the support of $\alpha(r)$, denoted by r_0. Let β_0 represent a characteristic breaking rate scale, and let α_0 represent the characteristic formation rate. Scale the distribution of junctions, ψ, by α_0/β_0, the stress by $S_0\alpha_0 r_0^5/\beta_0$, and the shear rate by the breaking rate. The dimensionless equations for the junction concentration and shear stress are

$$\gamma y_2 \frac{\partial \psi}{\partial y_1} = \alpha(|\boldsymbol{y}|) - \beta(|\boldsymbol{y}|)\,\psi \tag{A.1}$$

$$\sigma_{12} = \int y_1 y_2\, \psi(\boldsymbol{y})\; d\boldsymbol{y}. \tag{A.2}$$

Because of symmetry, the equation for ψ only need be solved for $y_2 > 0$, and so it is assumed below that y_2 is positive. For notational convenience, define

$$r_s = \sqrt{s^2 + y_2^2 + y_3^2}, \tag{A.3}$$

and the functions b and b_1 by

$$b(y_2, y_3) = \sqrt{1 - y_2^2 - y_3^2} \tag{A.4}$$

$$b_1(y_3) = \sqrt{1 - y_3^2}. \tag{A.5}$$

Equation (A.1) can be integrated to give

$$\psi = \begin{cases} \displaystyle\int_{-b}^{y_1} \frac{\alpha(r_\xi)}{\gamma y_2} \exp\!\Big(-\frac{1}{\gamma y_2}\int_\xi^{y_1} \beta(r_s)\; ds\Big)\, d\xi, & \text{for } |y_1| \le b \\ \displaystyle\int_{-b}^{b} \frac{\alpha(r_\xi)}{\gamma y_2} \exp\!\Big(-\frac{1}{\gamma y_2}\int_\xi^{y_1} \beta(r_s)\; ds\Big)\, d\xi, & \text{for } y_1 > b \\ 0 & \text{otherwise} \end{cases} . \tag{A.6}$$

Split σ_{12} into the stress due to short bonds and the stress due to long bonds, where short bonds are defined as those whose length is less than 1, which is the radius of support of the formation function.

$$\sigma_{12} = \sigma_{12}^s + \sigma_{12}^l = \int_{r<1} y_1 y_2 \, \psi \, d\boldsymbol{y} + \int_{r\geq 1} y_1 y_2 \, \psi \, d\boldsymbol{y}. \tag{A.7}$$

The stress is split in this manner because short and long bonds have different asymptotic behaviors. If fact, for short bonds the form of the breaking rate need not be specified to determine the leading order behavior of the stress.

A.1 Short Bonds

First we determine the contribution from short bonds to the shear stress. We now show that the shear stress due to short bonds is order γ^{-1}, making an order γ^{-2} contribution to the shear viscosity.

Using the expression for ψ from (A.6) in the definition for short bonds gives

$$\sigma_{12}^s = 2\int_{-1}^{1}\int_{0}^{b_1}\int_{-b}^{b}\int_{-b}^{y_1} \frac{y_1 \alpha\left(r_\xi\right)}{\gamma} \exp\!\left(-\frac{1}{\gamma y_2}\int_{\xi}^{y_1} \beta\left(r_s\right)\, ds\right) d\xi dy_1 dy_2 dy_3. \tag{A.8}$$

Because the formation rate and breaking rate must be finite for short bonds, it is sufficient to take α and β equal to one to determine the order of the stress due to short bonds. This could be argued formally by bounding these functions above and below by piecewise constant functions, but this is unnecessary for the present discussion.

With α and β set to one, equation (A.8) simplifies to

$$\sigma_{12}^s = 2\int_{-1}^{1}\int_{0}^{b_1}\int_{-b}^{b} y_1 y_2 \left(1 - \exp\left(-\gamma^{-1}\,\frac{y_1 + b}{y_2}\right)\right) dy_1 dy_2 dy_3 \tag{A.9}$$

Note that for any finite K,

$$1 - \exp\left(\gamma^{-1}K\right) = \gamma^{-1}K + \mathcal{O}\left(\gamma^{-2}\right). \tag{A.10}$$

It is tempting to expand the integrand in (A.9) in a Taylor series, but this cannot be done because y_2 is not bounded away from zero. However, it is shown in [16] that this problem can be circumvented by splitting the domain of integration so that a Taylor series can be applied over part of the domain. Then taking the proper limit,

$$\sigma_{12}^s = \mathcal{O}\left(\gamma^{-1}\right). \tag{A.11}$$

Therefore the shear viscosity for short bonds is order γ^{-2}. This result is especially relevant when there are no long bonds present, as would be the case if

the bonds had a maximal length at which they break. It is shown in the next section that the shear viscosity for long bonds is lower order, and therefore the short bonds do not contribute to the leading order behavior of the viscosity.

A.2 Long Bonds

For long enough bonds, we consider breaking rates of the form

$$\beta = (\kappa_L r)^n + \text{lower order terms.} \tag{A.12}$$

Since we have assumed that the formation rate has compact support and the flow is only in the y_1-direction, the largest contribution to the length of a long bond is from stretching in the y_1-direction. For simplicity we assume that

$$\beta = (\kappa_L y_1)^n . \tag{A.13}$$

This assumption is not necessary to perform the analysis [16], but it greatly simplifies the computation and the leading order result is unchanged.

For $y_1 > b$, using the breaking rate (A.13), the distribution of the junctions given by (A.6) can be expressed as

$$\psi(y_1, y_2, y_3) = \exp\left(\frac{-\kappa_L^n}{\gamma y_2 (n+1)}\left(y_1^{n+1} - b^{n+1}\right)\right)\psi(b, y_2, y_3) . \tag{A.14}$$

The shear stress due to long bonds is

$$\sigma_{12}^l = 2\int_{-1}^{1}\int_{0}^{b_1}\int_{b}^{\infty} y_1 y_2\, \psi(y_1, y_2, y_3)\; dy_1 dy_2 dy_3 \tag{A.15}$$

$$= 2\int_{-1}^{1}\int_{0}^{b_1} \exp\left(\frac{\kappa_L^n b^{n+1}}{\gamma y_2 (n+1)}\right)\; y_2 \psi(b, y_2, y_3)\; I_1\, dy_2 dy_3, \tag{A.16}$$

where

$$I_1 = \int_b^\infty y_1 \exp\left(\frac{-\kappa_L^n y_1^{n+1}}{\gamma y_2 (n+1)}\right)\; dy_1. \tag{A.17}$$

The general form of $\psi(b, y_2, y_3)$ is

$$\psi(b, y_2, y_3) = \frac{1}{\gamma y_2}\int_{-b}^{b} \alpha(r_\xi) \exp\left(\frac{-1}{\gamma y_2}\int_\xi^b \beta(r_s)\; ds\right) d\xi. \tag{A.18}$$

To leading order

$$\psi(b, y_2, y_3) \sim \frac{1}{\gamma y_2}\int_{-b}^{b} \alpha(r_\xi)\; d\xi, \tag{A.19}$$

where we have taken the exponential to be one to leading order. As with short bonds this approximation can be shown to be valid even though y_2 is not

bounded away from zero. Similarly, we take the exponential appearing in the integrand of (A.16) to be one to leading order by the same arguments, so that

$$\sigma_{12}^{l} \sim 2 \int_{-1}^{1} \int_{0}^{b_1} \frac{1}{\gamma} \int_{-b}^{b} \alpha\left(r_{\xi}\right)\, d\xi\, I_1\, dy_2 dy_3. \tag{A.20}$$

Using Watson's Lemma [24] the leading order behavior of I_1 is

$$I_1 \sim \frac{\kappa_L^{-2n/(n+1)}}{(n+1)^{(n-1)/(n+1)}} \Gamma\left(\frac{2}{n+1}\right) \gamma^{2/(n+1)} y_2^{2/(n+1)}. \tag{A.21}$$

Combining (A.20) and (A.21) gives

$$\sigma_{12}^{l} \sim \gamma^{(1-n)/(1+n)}\, \frac{\kappa_L^{-2n/(n+1)}}{(n+1)^{(n-1)/(n+1)}} \Gamma\left(\frac{2}{n+1}\right) \int_{r<1} y_2^{2/(n+1)} \alpha(r)\, d\boldsymbol{y}. \tag{A.22}$$

The integral may be simplified to

$$\int_{r<1} y_2^{2/(n+1)} \alpha(r)\, d\boldsymbol{y} = 4\pi \frac{(n+1)}{(n+3)} \int_0^1 \alpha(r) r^{(2n+4)/(n+1)}\, dr. \tag{A.23}$$

Converting back to dimensional quantities and extending the upper limit of integration gives the proportionality constant (26). The leading order term of the stress is proportional to $\gamma^{(1-n)/(1+n)}$, and the leading order term for the shear viscosity is proportional to $\gamma^{-2n/(n+1)}$.

References

[1] M. S. Green, A. V. Tobolsky, A new approach to the theory of relaxing polymeric media, J. Chem. Phys. 14 (1946) 80–92.

[2] R. G. Larson, Constitutive Equations for Polymer Melts and Solutions, Butterworth, Stoneham, MA, 1988.

[3] M. Yamamoto, The viscoelastic properties of network structure, I. General formalism, J. Phys. Soc. Jpn. 11 (1956) 413–421.

[4] M. Yamamoto, The viscoelastic properties of network structure, II. Structural viscosity, J. Phys. Soc. Jpn. 12 (1957) 1148–1158.

[5] G. G. Fuller, L. G. Leal, Network models of concentrated polymer solutions derived from the Yamamoto network theory, J. Polym. Sci., Polym. Phys. Ed. 19 (1981) 531–555.

[6] F. Petruccione, P. Biller, A numerical stochastic approach to network theories of polymeric fluids, J. Chem. Phys. 89 (1988) 577–582.

[7] M. Laso, H. Öttinger, Calculation of viscoelastic flow using molecular models: the CONNFFESSIT approach, J. Non-Newton. Fluid Mech. 47 (1993) 1–20.

[8] P. Halin, G. Lielens, R. Keunings, V. Legat, The Lagrangian particle method for macroscopic and micro-macro viscoelastic flow computations, J. Non-Newton. Fluid Mech. 79 (1998) 387–403.

[9] N.-T. Wang, A. L. Fogelson, Computational methods for continuum models of platelet aggregation, J. Comp. Phys. 151 (1999) 649–675.

[10] N. Phan-Thien, R. I. Tanner, A new constitutive equation derived from network theory, J. Non-Newton. Fluid Mech. 2 (1977) 353–365.

[11] J. Mewis, M. M. Denn, Constitutive equations based on the transient network concept, J. Non-Newton. Fluid Mech. 12 (1983) 69–83.

[12] F. Tanaka, S. F. Edwards, Viscoelastic properties of physically cross-linked networks. Transient network theory, Macromolecules 25 (1992) 1516–1523.

[13] A. Vaccaro, G. Marrucci, A model for the nonlinear rheology of associating polymers, J. Non-Newton. Fluid Mech. 92 (2000) 261–273.

[14] A. L. Fogelson, Continuum models of platelet aggregation: Formulation and mechanical properties, SIAM J. Appl. Math. 52 (1992) 1089–1110.

[15] A. L. Fogelson, Continuum models of platelet aggregation: Mechanical properties and chemically-induced phase transitions, Cont. Math. 141 (1993) 279–293.

[16] R. D. Guy, A continuum model of platelet aggregation: Closure, computational methods, and simulation, Ph.D. thesis, University of Utah (2004).

[17] R. B. Bird, R. C. Armstrong, O. Hassager, Dynamics of Polymeric Liquids, 2nd Edition, Vol. 2, Wiley, New York, 1987.

[18] F. Tanaka, S. F. Edwards, Viscoelastic properties of physically crosslinked networks: Part 1. Non-linear stationary viscoelasticity, J. Non-Newton. Fluid Mech. 43 (1992) 247–271.

[19] R. I. Tanner, Engineering Rheology, 2nd Edition, Oxford, New York, 2000.

[20] M. Herrchen, H. C. Öttinger, A detailed comparison of various FENE dumbbell models, J. Non-Newton. Fluid Mech. 68 (1997) 17–42.

[21] R. Keunings, On the Peterlin approximation for finitely extensible dumbbells, J. Non-Newton. Fluid Mech. 68 (1997) 85–100.

[22] G. Lielens, P. Halin, I. Jaumain, R. Keunings, V. Legat, New closure approximations for the kinetic theory of finitely extensible dumbbells, J. Non-Newton. Fluid Mech. 76 (1998) 249–279.

[23] G. Lielens, R. Keunings, V. Legat, The FENE-L and FENE-LS closure approximations to the kinetic theory of finitely extensible dumbbells, J. Non-Newton. Fluid Mech. 87 (1999) 179–196.

[24] J. P. Keener, Principles of Applied Mathematics, 2nd Edition, Addison-Wesley, Reading, Mass., 1999.

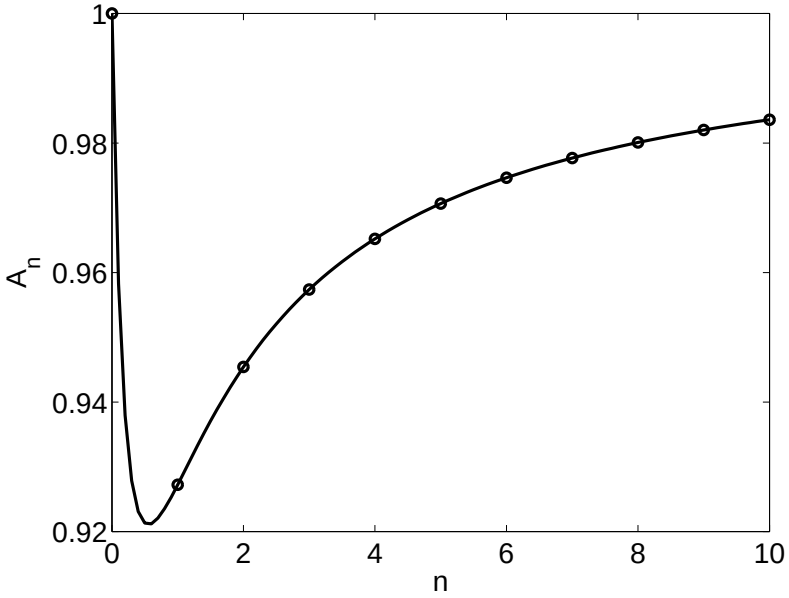

Fig. A.1. Plot of A_n for the Gaussian formation rate given by (101).

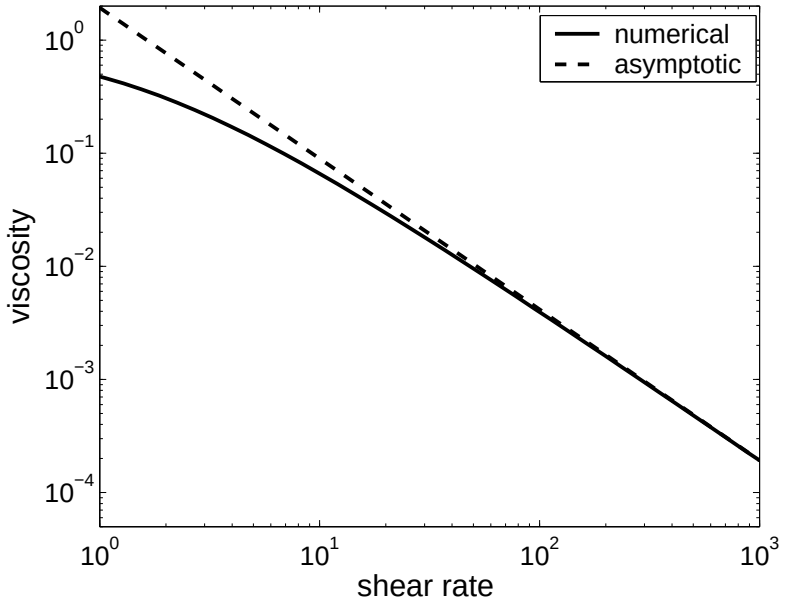

(a)

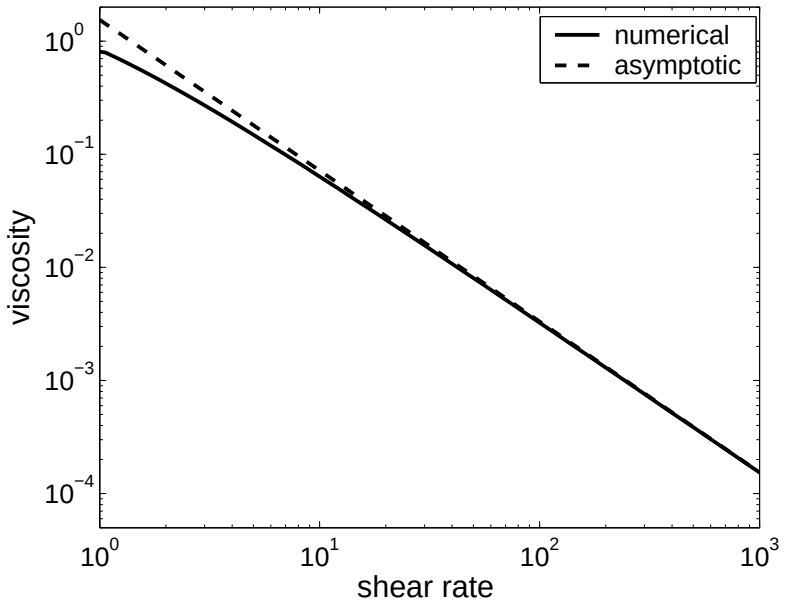

(b)

Fig. A.2. Comparing the asymptotic results for the shear viscosity with the computed solution for (a) the full model and (b) the PTT-vj closure.

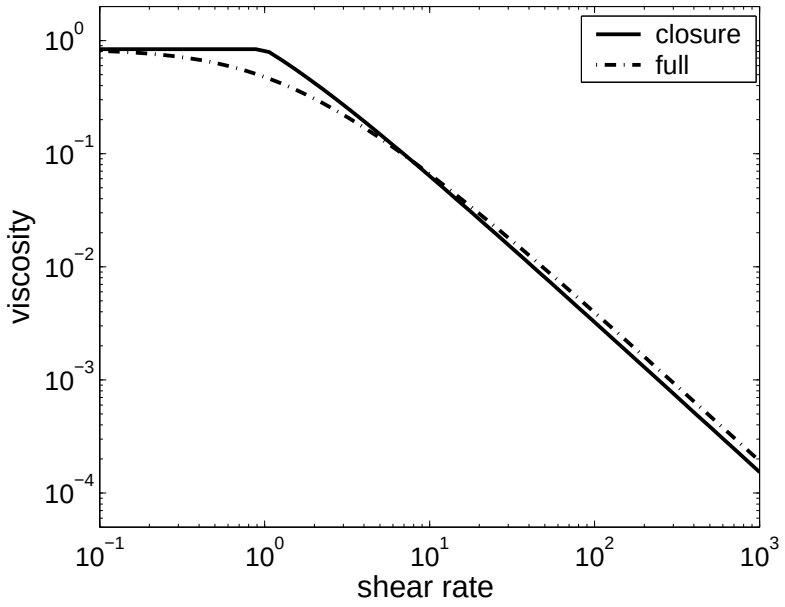

Fig. A.3. Comparison of the shear viscosity for the full model with breaking rate (107) and the PTT-vj closure with breaking rate (108) for a wide range of shear rates. The closure breaking rate results from simply replacing squared length with average squared length.

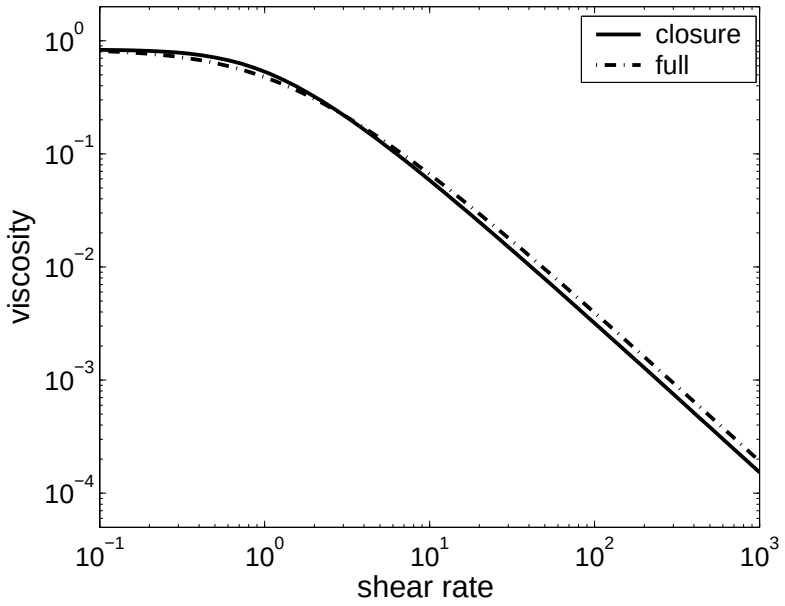

Fig. A.4. The closure model with breaking rate (112) is compared to the full model with breaking rate (107). The two models show excellent agreement for all shear rates.

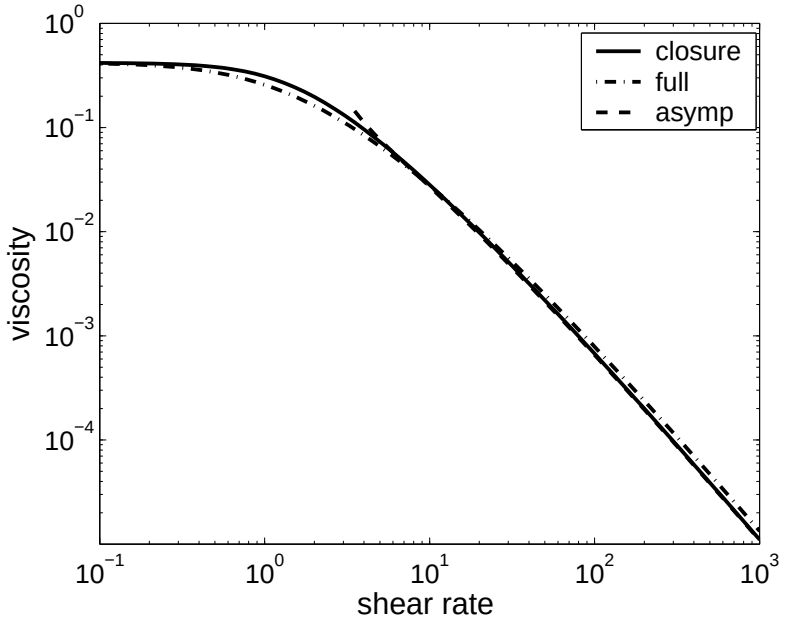

Fig. A.5. The closure model with the exponential breaking rate (114) is compared to the full model with the exponential breaking rate (113).

Table A.1
Results of the analysis for the PTT closure model

breaking rate	viscosity
$\beta = \left(\kappa_T \hat{T}\right)^n$	$\mu = \left(\frac{\sigma_0^{n+1}}{2^n \kappa_T^n}\right)^{1/(2n+1)} \gamma^{-2n/(2n+1)}$
$\beta = \exp\left(\kappa_T \hat{T}\right)$	$\mu = \left(\frac{\sigma_0}{2\kappa_T}\right)^{1/2} \gamma^{-1} \left(\ln\left((2\sigma_0\kappa_T)^{1/2}\gamma\right)\right) + o\left(\gamma^{-1}\left(\ln(\gamma)\right)^{1/2}\right)$
$\beta = \frac{1}{\kappa_T\left(T_{\max} - \hat{T}\right)}$	$\mu = \left(\frac{T_{\max}\sigma_0}{2}\right)^{1/2} \gamma^{-1} + o\left(\gamma^{-1}\right)$

Table A.2
Results of the analysis for the closure model PTT*

breaking rate	viscosity
$\beta = (\kappa_T T)^n$	$\mu = \left(\frac{a_2^{n+1}}{2^{2n}\kappa_T^{2n}}\right)^{1/(3n+1)} \gamma^{-4n/(3n+1)} + o\left(\gamma^{-4n/(3n+1)}\right)$
$\beta = \exp\left(\kappa_T T\right)$	$\mu = \left(\frac{a_2}{9\kappa_T^2}\right)^{1/3} \gamma^{-4/3} \left(\ln\left((3a_2\kappa_T)^{1/2}\gamma\right)\right)^{2/3} + o\left(\gamma^{-4/3}\left(\ln\left(\gamma\right)\right)^{2/3}\right)$
$\beta = \frac{1}{\kappa_T\left(T_{\max} - T\right)}$	$\mu = \left(\frac{a_2 T_{\max}^2}{4}\right)^{1/3} \gamma^{-4/3} + o\left(\gamma^{-4/3}\right)$

Table A.3
Results of the analysis for the closure model PTT-vj

breaking rate	viscosity
$\beta = \left(\kappa_L^2 T/z\right)^n$	$\mu = \left(\frac{a_0 a_2^{1/2n}}{2\kappa_L^2}\right)^{2n/(2n+1)} \gamma^{-4n/(2n+1)} + o\left(\gamma^{-4n/(2n+1)}\right)$
$\beta = \exp\left(\kappa_L^2\left(T/z\right)\right)$	$\mu = \frac{a_0}{2\kappa_L^2}\gamma^{-2}\left(\ln(\gamma) - \frac{1}{2}\ln\left(\frac{a_0}{2\kappa_L^2 a_2}\right)\right) + o\left(\gamma^{-2}\ln(\gamma)\right)$
$\beta = \frac{1}{\kappa_L^2\left(L_{\max}^2 - T/z\right)}$	$\mu = \left(\frac{a_0 L_{\max}^2 - 3a_2}{2}\right)\gamma^{-2} + o\left(\gamma^{-2}\right)$